Closed-Loop Neurostimulators: A Survey and A Seizure-Predicting Design Example for Intractable Epilepsy Treatment

Hossein Kassiri, *Member, IEEE*, Sana Tonekaboni, M. Tariqus Salam, *Member, IEEE*, Nima Soltani, Karim Abdelhalim, Jose Luis Perez Velazquez, and Roman Genov, *Senior Member, IEEE*

***Abstract*—First, existing commercially available open-loop and closed-loop implantable neurostimulators are reviewed and compared in terms of their targeted application, physical size, system-level features, and performance as a medical device. Next, signal processing algorithms as the primary strength point of the closed-loop neurostimulators are reviewed, and various design and implementation requirements and trade-offs are discussed in details along with quantitative examples. The review results in a set of guidelines for algorithm selection and evaluation. Second, the implementation of an inductively-powered seizure-predicting microsystem for monitoring and treatment of intractable epilepsy is presented. The miniaturized system is comprised of two mini-boards and a power receiver coil. The first board hosts a 24-channel neurostimulator system on chip [15] fabricated in a 0.13 μm CMOS technology and performs neural recording, on-chip digital signal processing, and electrical stimulation. The second board communicates recorded brain signals as well as signal processing results wirelessly. The multilayer flexible coil receives inductively-transmitted power. The system is sized at 2 $\times$ 2 $\times$ 0.7 cm^3 and weighs 6 g. The approach is validated in the control of chronic seizures *in vivo* in freely moving rats.**

***Index Terms*—Battery-less, brain implant, brain monitoring, closed loop, closed-loop SoC, chronic in-vivo experiments, diagnostics, epilepsy, implantable neurostimulator, inductive powering, intractable, multi-band radio, neural recording, neural stimulation, phase synchronization, seizure detection, system-on-chip, wireless implant.**

I. Introduction

ACCORDING to a report by World Health Organization, in 2007 neurological disorders were estimated to affect as many as a billion people worldwide, regardless of their age, sex, or geographical region [1]. This number is associated with age and is projected to grow rapidly due to increased life expectancy and reduced fertility.

Until this century, pharmacological solutions and brain surgery were the only two options available to patients with some of the most common neurological disorders such as epilepsy and Alzheimer's disease. Drugs often have limited overall therapy efficacy [2], commonly cause side-effects, and the patient develops resistance to them after a while. In addition, only a small fraction of patients are deemed to be candidates for brain surgery (e.g., 15% for epilepsy). This is because for many cases, the source of neurological disorder is close to a vitally-important part of the brain where a surgery could result in irreversible damage to patient's basic functionalities (e.g., movement, speech).

About a decade ago, electrical stimulation was demonstrated in multiple studies such as [3] and [4] as a promising alternative treatment for patients with Parkinson's disease and depression. Since then, many research groups have been working on both (a) improving and fine-tuning the technology for those disorders, and (b) developing and validating a comprehensive medical device for diagnosis and treatment of various other neurological disorders.

Unlike some diseases, such as Parkinson's, where stimulation pulse parameters (frequency, amplitude, width, etc.) and stimulation delivery location are the most important parameters for an effective treatment, for some other disorders the timing of pulse delivery is also of utmost importance. For instance, to stop an epilepsy seizure using electrical stimulation, it is widely believed that the seizure must be detected before its clinical onset, otherwise there is a very low chance to stop it [5]. This suggests that a brain activity monitoring feature is essential to be integrated in these devices to enable detection of a neurological event such as epilepsy seizure. The monitoring feature could initially be used for advisory applications, where the recorded brain activity is used to alert the patient/doctor about an upcoming event. One example is a device proposed in 2008 [6]. This epileptic seizure advisory system, records intracranial EEG signals through electrodes implanted between the skull and the brain surface. The signals are wirelessly transmitted to an external hand-held device that processes the data and transmits visual and audible warnings to the patient [7].

Manuscript received August 28, 2016; revised December 23, 2016; accepted April 4, 2017. Date of publication July 17, 2017; date of current version September 25, 2017. This paper was recommended by Associate Editor Z. Wang. *(Corresponding author: Hossein Kassiri.)*

H. Kassiri is with the Department of Electrical and Computer Engineering, University of Toronto, Toronto, ON M4s1e2, Canada, and also with the Department of Electrical Engineering and Computer Science , York University, Toronto, ON M3J 1P3, Canada (e-mail: hkasiri@gmail.com).

S. Tonekaboni, N. Soltani, K. Abdelhalim, and R. Genov are with the Department of Electrical and Computer Engineering, University of Toronto, Toronto, ON M4s1e2, Canada (e-mail: sana.tonekaboni@mail.utoronto.ca; nima@eecg.toronto.edu; karim@eecg.utoronto.ca; roman@eecg.utoronto.ca).

M. Tariqus Salam and J. L. Perz Velazquez are with the Brain and Behavior Program and Division of Neurology, Hospital for Sick Children, Toronto, ON M5G 1X8, Canada (e-mail: tariq@eecg.utoronto.ca; jose-luis.perez-velazquez@sickkids.ca).

Color versions of one or more of the figures in this paper are available online at http://ieeexplore.ieee.org.

Digital Object Identifier 10.1109/TBCAS.2017.2694638

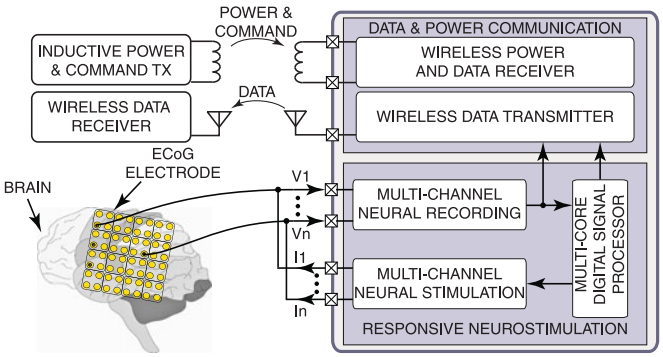

Fig. 1. Block diagram of a generic wireless closed-loop neurostimulator microsystem interfaced with a brain.

In addition to advisory applications, the output of the brain monitoring module could also be used to provide a timely feedback (e.g., electrical stimulation) to the brain to stop an undesired event. Such a configuration where the stimulation pulses are delivered only upon detection of an event, is the basis of closed-loop neurostimulator devices that have been investigated as a promising treatment alternative for millions of patients.

Fig. 1 shows the top-level block diagram of a wireless closed-loop neurostimulator connected to a human brain. As shown, the device includes multiple recording and stimulation channels and a digital signal processor. To make the system fully-implantable, recorded data must be communicated wirelessly and energy should be provided by a battery or through magnetic induction. Using a battery that is suitable for chronic experiments (i.e., can last a few months) increases the system weight and size significantly [8], [9]. Also if the system is implanted, a routine follow-up surgery is required once the battery is discharged [10]. On the other hand, inductive powering imposes no limitation on the system lifetime and can either be used to directly provide energy to the system or to recharge a smaller battery.

For a timely and effective responsive neuro-modulation feedback, both system's overall power dissipation and decision-making latency must be minimized. On-chip implementation of the signal processing unit delivers low latency, but comes at the cost of limited available computational power. As a result, out of many software-based algorithms that are reported for early detection of epileptic seizures, there are only some of them that fit within the power and area budget of an implantable SoC (system on chip). As a result developing a DSP that yields high sensitivity and specificity while keeping the number of features and classifier complexity to the minimum is one of the most challenging tasks in the design of closed-loop neurostimulators.

In addition to signal recording, processing and stimulation which are the core features of an implantable neurostimulator, there are other aspects that must be considered for a device that is intended for long-term use. Over the past decade, several implantable neural interface designs have been reported, each optimized to perform well for a specific targeted application [8], [9], [11]–[21]. However, chronic implantation constraints such as longevity and ease of implantation and use are often ignored. A microsystem that is designed for long-term use (monitoring or treatment), not only must perform well in terms of brain neural signal acquisition and processing, but also should have a small form factor, be fully wireless, and operate fully-autonomous. Additionally, both of the wireless links for data and power must have a reasonable range (>10 cm) to ensure the ease of use, while the specific absorption rate (SAR) is kept below the safety-permitted limit [22].

In this paper, first, we review various commercially-available implantable neurostimulators (both open-loop and closed-loop devices) and compare them in terms of their targeted application, physical size, system-level features, and performance as a medical device. The review establishes the superiority of closed-loop devices to open-loop ones, due to the seizure detection algorithm integrated into their monitoring feature. Inevitably, the next section of the paper is an extensive discussion on signal processing algorithms for detection of neurological events. The discussion starts with introducing the practical requirements that must be taken into account, followed by a thorough review of state of the art algorithms categorized by the type of features they use (e.g., univariate or bivariate, time-domain or frequency-domain, etc.), and the type of classifier they employ (e.g., thresholding or machine learning). Due to the importance of hardware implementation as discussed previously, the review is followed by introducing and comparing state of the art SoCs with an on-chip signal processing unit for detection of a neurological event. The review results in a set of guidelines for algorithm selection and validation.

In the second part of the paper, an epilepsy seizure detection algorithm is selected and is integrated into an implantable device described below. The device is a 24-channel inductively-powered implantable microsystem for neural signal monitoring, on-chip signal processing and biphasic current-mode stimulation. A 12 mm^2 0.13 μm CMOS SoC performs the core of signal recording, processing and stimulation [15]. The system transmits diagnostic data to the outside of the body wirelessly and receives its energy directly from an inductive powering link several centimeters away. The system's efficacy in epileptic seizure detection and abortion is validated using a statistically-important database (to validate the algorithm efficacy) as well as in an in-vivo online experiment on freely-moving rats with temporal lobe epilepsy (to validate the device performance). This section extends on an earlier report of the principle and demonstration in [26], and offers a more detailed analysis of the design as well as a review of the state-of-the-art and commercially-available implantable devices. It also provides a comprehensive discussion on requirements and trade-offs that must be considered during the design of an implantable wireless neurostimulator, with a special focus on on-chip implementation of the DSP unit. Additional experimental results characterizing the circuit implementation and in-vivo validation are also included.

The rest of the paper is organized as follows. Section II reviews commercially-available wireless brain neurostimulators. Section III reviews and compares various seizure prediction algorithms and compares the performance of state of the art hardware implementation of such algorithms. Section IV summarizes different design challenges of an implantable wireless neurostimulator, and discusses the VLSI architecture of the example device. Section V presents system's electrical experimental results. Section VI presents in-vivo online animal epilepsy seizure detection and treatment results.

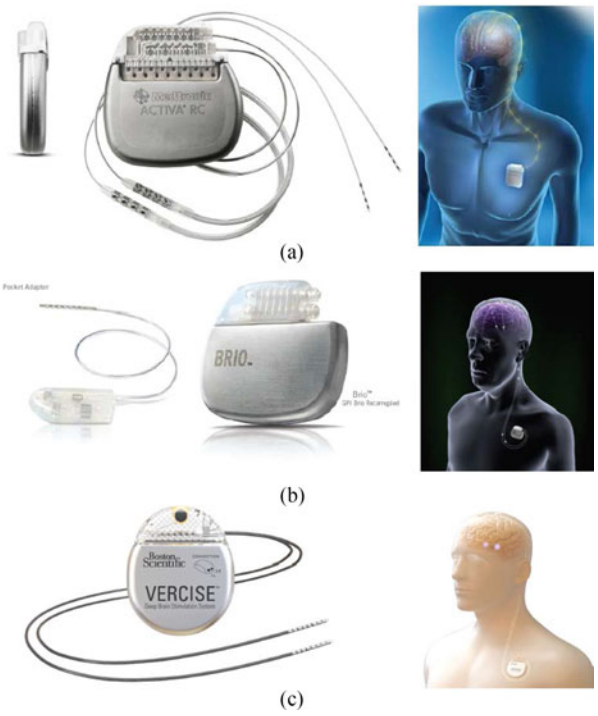

Fig. 2. Three commercially-available open-loop battery-powered neurostimulators: (a) Medtronic Activa RC [32], (b) St. Jude Brio [33], and (c) Boston Scientific Vercise PC [30].

II. A Survey on Commercial Neurostimulators

Following several years of research on the development of implantable neural interfaces, some commercial neurostimulator devices have recently become available. They can be categorized into two main groups of open-loop (periodic pulse trains) and closed-loop (responsive) stimulators. From another point of view, currently-available neurostimulation devices can be categorized as vagus nerve stimulators (VNS) or deep brain stimulators (DBS). In VNS therapy, pulses are delivered indirectly to the brain through vagal nerve, while in DBS, stimulation is directly applied to the brain cells. Both methods are shown to be effective for treatment of neurological disorders such as drug-resistant epilepsy or Parkinson's disease [27], [33].

A. Open-Loop Neurostimulators

Open-loop neurostimulators are devices that deliver preprogrammed periodic electrical pulses to the brain via implanted electrodes. A physician can program the device based on the severity of the patient's disease to determine how often and how intense these pulses need to be. A list of key open-loop neuromodulators currently available on the market is presented below.

1) Medtronic: Medtronic has offered a series of open loop brain stimulators that target diseases such as essential tremor and Parkinson's disease. For instance, the Activa RC (Rechargeable) shown in Fig. 2(a) is a 40 gram device, typically implanted subcutaneously near the clavicle, and connected to leads implanted in the brain. After being programmed, it delivers controlled electrical pulses to precisely-targeted areas of the brain [32]. This deep brain stimulation is done both in current and voltage modes, through up to 4 electrodes. The device is battery-powered and the battery lasts up to 9 years depending on the frequency of the stimulations. It comes with a patient programmer device that checks the battery status of the pulse generators and allows the physicians to adjusts the therapy wirelessly. The transmission is with a carrier frequency of 175 kHz, and an output level of -48 dBμV/m.

2) St. Jude: St. Jude medical has also introduced the Brio, shown in Fig. 2(b), with an advanced rechargeable technology that functions for at least 10 years [33]. The device is designed for the treatment of Parkinson's disease and its biggest difference compared to other devices with similar application is the use of constant current pulse delivery [34]. It supports 2 leads and 16 contacts, and has three options for the current path: monopolar, bipolar, and multipolar. It is implanted under the skin of the upper chest and sends the impulses through wire leads that attach the device to electrodes implanted in the brain.

3) Boston Scientific: Another Implantable pulse generator is the Vercise PC (Primary Cell) shown in Fig. 2(c), from Boston Scientific. This 16-contact implantable pulse generator features a multiple independent current control (MICC) system with current steering technology, which allows precise control of the stimulation field [30]. The user friendly environment of its programming software allows for precise programming of all the parameters of the stimulation. It can also report a graphical summary of the therapeutic benefits and side effects at a given position along the DBS lead [29].

B. Closed-Loop Neurostimulators

Despite their benefits, open-loop neurostimulators operation could be considered blind due to the lack of a brain monitoring feature. This causes several issues, both in terms of patient's safety, and the device longevity and efficacy. For instance, long-term continuous neurostimulations is shown to cause habituation and changes in the neural chemistry, which can result in an ineffective treatment after a while [31]. Also, since these devices deliver stimulations constantly, they subject the patient to excess pulses which reduces the overall efficiency of the open-loop technique, and also results in a faster battery depletion. Additionally, for many neurological disorders such as epilepsy, an effective stimulation only takes place if it is triggered at the right time.

To address mentioned shortcomings, closed-loop neurostimulators have been investigated during the past years, and only recently, a few of such devices are introduced to the market. Closed-loop neurostimulators constantly monitor patient's neuro-physiological activity to detect/predict a neurological event of interest that is likely to happen. Only when a particular event is detected, the stimulation is triggered and pulses are delivered to the neural system. Below are some of the commercially-available closed-loop neurostimulators.

1) Neuropace: The Neuropace RNS (Responsive Neurostimulator), shown in Fig. 3(a), is a closed-loop device designed for epilepsy treatment. This device is $28 \times 60 \times 7.7$ mm^3 and weighs about 17 grams and is powered by a battery with a

Fig. 3. (a) Neuropace RNS responsive neurostimulator [37]. (b) Medtronic Activa PC+S closed-loop neurostimulator. (c) LivaNova Aspire SR closed-loop neurostimulator [35].

longevity around 2 to 3.5 years [37]. Unlike other closed-loop devices, it is implanted in the brain and delivers pulses in a DBS fashion, upon detection of an upcoming epilepsy seizure [38]. Once stimulation is triggered, current-regulated biphasic pulses with $40-1000$ μs width are delivered to 8 electrodes implanted in the brain [37]. At the same time, the recorded brain data are transferred wirelessly to the patient's data management system. The physicians use a programmer to control the stimulator and a wand to monitor patient's brain activity. The wand works with a short-range wireless radio frequency link. Wireless transmission is done in 20–50 kHz range with effective radiated power of 224 pW or less. Tables I and II compare various characteristics of different types of open-loop and closed-loop neurostimulators, respectively.

2) Medtronic: Another product introduced by Medtronic is the Activa PC+S (Primary Cell + Sensing), shown in Fig. 3(b). This new device with similar physical and electrical stimulation characteristics to Activa PC, has the added feature of recording brain activities, and sending stimulation pulses accordingly. Implanted subcutaneously near the clavicle, it is able to monitor brain activities to see how patients respond to the therapy and allows the doctors to improve the therapy. In addition to programming the device, the programmer also interrogate information such as battery status from the device [36].

3) LivaNova: LivaNova (previously Cyberonics) has recently introduced the Aspire SR (Seizure Response), shown in Fig. 3(c). This device constantly monitors the heart beat and delivers stimulation pulses when it detects a rapid heart rate raise. The ECG (ElectroCardioGram) sensor and the pulse generator, implanted in the chest area, are connected to the vagus nerve, and deliver pulses through lead wires. This 25-grams generator is programmed using a wireless remote wand. The device receives programming signals from the wand and transmits back telemetry information. The power source is a lithium carbon monofluoride battery with a lifetime of approximately 4 to 7 years, depending on the frequency of the pulses [35].

C. Commercial Devices Review Conclusion

Reviewing commercially-available neurostimulators reveals that closed-loop devices generally outperform open-loop ones in treatment of targeted neurological disorder, mainly due to the signal processing feature integrated into them. The critical role of the signal processing unit motivates for studying various available algorithms in terms of their performance (accuracy and latency) and their feasibility for hardware implementation. Hardware implementation of the algorithm is important to achieve real-time responsive stimulation, but makes computational expensiveness one of the deciding factors. The review results in a framework for algorithm selection and validation.

III. Hardware Implementation of an Early Seizure Detection Algorithm

In this section, to compare different detection algorithms, epilepsy seizure is selected as an example for the targeted neurological event. Being the third most popular neurological disorder, with 15% of the patients refractory to the current treatment options (drugs and surgery) neurostimulators are expected to be crucial in improving quality of life in many epileptic patients. First we go over the main requirements for an epilepsy seizure detection algorithm. Next, a thorough review of different categories of algorithms are presented. The review is followed by a conclusion regarding the signal features and classification methods. The section ends with a review of state of the art hardware implementation of signal processing algorithms for detection of neurological disorders.

A. Practical Requirements

It is almost four decades that algorithms/methods for epileptic seizure detection are sought. Early success seemed to be achieved during first few years of investigation by many groups. However, after about two decades, researchers found methodological mistakes in the performance evaluation and statistical significance of then-existing algorithms, which stopped them from pursuing their implementation on a therapeutic device. Studies such as [39]–[41] challenged the reliability and reported results by previous works, and showed that the optimistic detections/predictions were made due to various methodological caveats. In short, the major issue was that the performance evaluation was made on over-optimized algorithms applied to small selected dataset.

In 2007, Mormann et al performed a thorough review on seizure prediction algorithms [42]. They concluded that to evaluate methodological quality of a seizure detection algorithm, first, it must be tested on unselected continuous long-term recordings

TABLE I
STATE-OF-THE-ART COMMERCIAL OPEN-LOOP NEURAL STIMULATION SYSTEMS

	Activa RC Fig. 2(a)	Brio Fig. 2(b)	Vercise PC Fig. 2(c)
Manufacturing company	Medtronic	St. Jude	Boston Scientific
Release Date	May 2009	June 2015	September 2015
Stimulation Site	Deep Brain Stimulation	Deep Brain Stimulation	Deep Brain Stimulation
Targeted Application	Parkinson's Disease Essential Tremor	Parkinson's Disease Essential Tremor	Parkinson's disease Dystonia, Essential Tremor
Size (mm^3)	$54 \times 54 \times 11$	$48 \times 53 \times 10$	22
Weight (grams)	40	29	N/R
No. of Stim. Channels	4	16	16
Output Current (mA)	0.25–5	0–12.75	0.1–20
Output Voltage (V)	0–10.5	0–6.5	N/R
Frequency (Hz)	2–250	2–240	2–225
Pulse Width (μs)	60–450	50–500	10–450
Battery Longevity (years)	9	10	25 (Rechargeable)
Battery Type	Rechargeable	Rechargeable	Non-rechargeable/Rechargeable
Implant Site	Chest Area	Chest Area	N/R
Recorded Data Monitoring	Wireless	Wireless	Wireless

N/R: Not Reported

TABLE II
STATE-OF-THE-ART COMMERCIAL CLOSED-LOOP NEURAL STIMULATION SYSTEMS

	RNS Fig. 3(a)	Activa PC+S Fig. 3(b)	Aspire SR Fig. 3(c)
Manufacturing Company	Neuropace	Medtronic	LivaNova
Release Date	November 2013	January 2013	June 2015
Stimulation Site	Deep Brain Stimulation	Deep Brain Stimulation	Vagus Nerve Stimulation
Targeted Application	Drug-Resistant Epilepsy	Parkinson's Disease	Epilepsy
Size (mm^3)	$28 \times 60 \times 7.7$	$65 \times 49 \times 15$	14
Weight (grams)	16	67	25
No. of Stim. Channels	8	4	N/R
Output Current (mA)	6–11.5	0–25.5	0–3.5
Output Voltage (V)	6-12	0–10.5	N/R
Frequency (Hz)	1–333	2–250	1–30
Pulse Width (μs)	40-1000	60–450	130–1000
Battery Longevity (years)	2–3.5	9	4–7
Battery Type	Non-rechargeable	Rechargeable	Non-rechargeable
Implant Site	In the Skull, Under the Scalp	Chest Area	N/R
Recorded Data Monitoring	Wireless	Wireless	Wireless

N/R: Not Reported

covering several days of EEG, to capture all the physiological states of a patient. Second, performance must be evaluated based on not only the sensitivity, but also the specificity with respect to the applied prediction horizon. Finally the results must be tested using a statistical validation method to prove that it is above the chance level.

B. Seizure Detection Algorithms

Over the past 15 years, several seizure detection algorithms have been reported with consideration of the above requirements [55]–[65]. Both analytical and machine-learning-based classifiers are investigated and relative success is achieved in some cases of both approaches. Algorithms can also be categorized based on their feature selection. In terms of spatial specificity, both univariate [43]–[46] and multi-variate [47]–[53] algorithms are reported. By adding spatial information to the inputs, the algorithms are able to compare the same features for different locations on the brain, and yield a generally higher detection accuracy.

Due to the importance of feature selection for an accurate seizure detection, here we categorize reported algorithms based on the nature of signal features they extract prior to classification.

1) Time-Based Methods: A major group of algorithms are based on time-domain features and pattern recognition. In [55] spatiotemporal correlation is utilized to perform seizure prediction. The authors use delay correlation and covariance matrices that are computed at different delays. Prior to that, principal component analysis is performed to choose subject-specific top features to be used for correlation analysis. Finally a support vector machine is used to perform classification. The algorithm is tested on Freiburg dataset and achieves $86-95\%$, with 1.68–0.72 false positives per day.

In [56], the authors have investigated early seizure prediction by monitoring the changes in neuronal spiking rate during the pre-ictal period. After optimizing the threshold value for each patient in the Freiburg dataset, they have achieved 72.7% sensitivity with 2.64 false positives per day (50 minute seizure prediction horizon). In [57], a time-domain pattern recognition technique is used to detect occurence of specific patterns within the recorded EEG data. Freiburg dataset is used and a sensitivity of 67% is reported with approximately 1 false prediction per day (20 min prediction horizon).

A major group of time-based detection algorithms work based on signal's instantaneous phase when filtered to a certain frequency range. Phase synchronization received an increasing attention when it was shown to outperform other multi-variate algorithm in a comparative study [42]. In [58] mean phase coherence is utilized as a seizure indicator that experiences a sudden decrease before the seizure onset. Also in [59], another phase-based parameter, bivariate synchrony, is used for seizure detection. In addition to evaluating the algorithm with typical parameters suggested in previous studies such as [60], the authors also investigated the effect of averaging window length, data smoothing, and seizure prediction horizon. The authors report a highest sensitivity of 88%, but with false positive rate of 0.64-4.69 per hour.

2) Frequency-Based Methods: Spectral information extracted from the recorded EEG signals are also used in several studies to perform epileptic seizure detection. In [61] eight frequency bands of the recorded EEG signals are utilized for spectral power calculations. After preprocessing and normalization of the data, best features were selected and fed to a cost-sensitive support vector machine to classify between pre-ictal and inter-ictal states. High sensitivity of 98.3% with an average of 7 false positives per day is achieved.

In [62] the authors have calculated wavelet energy and entropy to differentiate between pre-ictal and inter-ictal states. To achieve best results, data pre-processing is done to select the best discriminating channels for each patient. An average sensitivity of 85% is reported while having an average 2.4 false positives per day, with seizure prediction horizon of 36 minutes.

In [63] spectral power of different EEG bands are used again on signals from the EPILEPSIAE database. Signal from six recording sites are analyzed and spectral power ratio is used as the discriminating parameter for seizure prediction. All possible ratios are calculated among 5 standard EEG bands, and non-important ones are removed prior to classifications. An SVM classifier is used for classification, yielding an average sensitivity of 78.36% with 3.6 false positives per day, while seizure prediction horizon was slightly higher longer than 33 minutes.

C. Algorithm Review Conclusions

Judging from the studies reviewed above and many more published works, some general conclusions could be made regarding different aspects of a seizure prediction algorithm. Comparing works with univariate and multivariate features shows that the most success is achieved when both types of measures are utilized. This is also confirmed in [64] where several measures are studies and compared. In terms of type of features used, none of time-based or frequency-based features demonstrate superiority, and their results are comparable, which suggests using a combination of both types, which might improve seizure prediction performance at higher computation cost.

Comparing studies that have used the same (or similar) features for prediction with significantly different outcome (e.g., [65] and [59]), suggests that features could have various effectiveness on different patients, and to achieve the best outcome, feature selection must be performed for each patient.

Perhaps the most interesting conclusions from reviewing many seizure prediction studies are: (a) while increasing number of features used for classification increases the demanded computational power, it does not necessarily improve classification results. In fact there are many algorithms with very few features that perform comparable to several-feature counterparts. (b) Results from threshold-based and AI-(artificial Intelligence) based algorithms are also comparable.

Taking all the studies into consideration, it can be concluded that for the best outcome, high-cost approaches such as increasing the number of temporal, spatial, or spectral features, and implementing a very advanced machine-learning-based classifier will not be as rewarding as selecting and combining the right patient-specific features. Once the right features are selected, a simple thresholding could yield a highly-accurate, yet low-cost classifier.

Finally, to be able to perform reliable clinical trials for development of a therapeutic device, the algorithm must be fully integrated into a chronically-implantable device that can perform recording and signal processing over a long ($>$1 month) period of time.

D. Hardware Implementation Review

As discussed previously, clinical requirements such as low-latency detection and on-time reaction to an upcoming neurological event such as epilepsy seizure necessitate hardware implementation of the event detection/prediction algorithm in a therapeutic device. Along with benefits, hardware implementation of a signal processing algorithm comes with challenges due to the tight size and energy budget associated with an implantable device. Therefore, computation power, algorithm complexity, power consumption, and scalability of area and power become important design parameters that must be taken into account. This introduces a trade-off between above parameters and seizure detection performance (sensitivity, specificity, and latency).

Similar to the studies done on software implementation of seizure detection algorithms, there is a great amount of research effort on low-power compact hardware implementation of such algorithms [11], [66]–[72]. Table III compares recently-published brain-interface SoCs with a signal processing unit integrated in them for neurological event detection. The listed devices are designed for detection of various neurological events, have a wide range of channel count (1 to 128), and some of them are equipped with closed-loop electrical stimulation unit for neuromodulation. The table also lists different extracted features and conducted algorithms prior to classification, and the signal processing engine used. For classification, both thresholding and machine-learning-based algorithms are reported.

IV. Design Example

Using the conclusions made in the previous Section III-C, a phase-based seizure detection algorithm is selected for on-chip implementation. The algorithm is implemented on a silicon chip

TABLE III
STATE-OF-THE-ART BRAIN-IMPLANTABLE SOCS WITH INTEGRATED DSP FOR NEUROLOGICAL EVENT DETECTION

Specifications	[66] JSSC 2008	[67] TNSRE 2009	[68] VLSI 2010	[69] JSSC 2010	[11] JSSC 2011	[70] JSSC 2013	[71] JSSC 2014	[72] TCAS-II 2015	THIS WORK
Tech. (μm)	0.8	0.35	0.09	0.18	0.35	0.18	0.18	0.18	0.13
Area (mm^2)	18	65	14.8	6.25	10.9	25	13.47	–	12
Supply (V)	1.8	3.3	1	1.0	1.5	1.8	1.8-10	0.8	1.2
Power Diss. (mW)	0.02	6	0.253	0.077	0.375	–	2.8	0.017	1.3
Number of Rec. Channels	4	128	16	1	4	8	8	16	24
SIGNAL PROCESSING	✓	✓	✓	✓	✓	✓	✓	✓	✓
DSP	Analog	Feature extraction	Programmable RISC	Feature extraction	Spike discriminator	Feature extraction	Feature extraction	Feature Extraction	Tri-core CORDIC
Univariate Feature	Mag	Spike peaks & derivative peaks	Chaoticity Energy	Spectral power	Temporal amp. var.	Spectral temporal variations	Spectral power & Entropy	Coastline	Mag. & Phase
Bivariate Feature	✗	✗	Cross correlation	✗	✗	Spectral spatial variations	✗	✗	Phase Synchrony
Classifier	Thresholding	Thresholding	✗	SVM	Thresholding	SVM	LLS	Thresholding	Thresholding
NEURAL STIMULATION	✓	✗	✗	✗	✓	✗	✓	✗	✓
# of Stim. Channels	1	–	–	–	4	–	1	–	24
Current Range (mA)	–	–	–	–	0-0.1	–	0.03	–	0.01-1
IN-VIVO RESULTS	✗	✗	✗	✗	✓	✗	✓	✗	✓
Sensitivity (%)	–	–	–	–	–	–	92	–	88-96
False Positive Rate (/hr)	–	–	–	–	–	–	–	–	0.03

as a component of an implantable device, making it ready for in-vivo experiments on rodent animal models for epilepsy. Testing on such models is a standard step prior to validation experiment on human primates.

We have previously reported a multi-channel neurostimulator SoC in [15]. The SoC is equipped with multiple recording and stimulation channels, and includes a synchrony-based signal processing unit for early epileptic seizure detection (thus seizure predictive). It is powered using a wired connection and can transmit data within several centimeters. For electrical measurements, a bulky (4.3×4.3 cm^2) packaged (PGA-209) version of the SoC was mounted on a large bench-top board, controlled by an Altera Cyclone III FPGA, and wireless transmission was done using a monopole antenna. The large form factor and high-power peripherals, made the system in [15] non-viable for chronic in-vivo experiments or clinical trials.

To make the system implantable and fully-autonomous, the SoC must be directly bonded to a PCB (avoiding any bulky package), and all the peripheral circuits must be either removed or replaced with low-power smaller versions to save area. As a result, the digital controller implemented on the FPGA must be redesigned to fit inside an ultra-low-power FPGA that has $\sim$10 times fewer logic elements (e.g., Actel IGLOO). Additionally, since everything must fit within a 2 cm^3 implant, the antennas must be redesigned and replaced with planar antennas implemented on the board. Finally, to be fully implantable while avoiding a bulky battery, power is preferred to be provided inductively.

A. System Architecture

Fig. 4(a) shows a system block diagram of the miniaturized implantable closed-loop neurostimulator. The system is comprised of a receiver coil, a wireless interface board and a neurostimulator board. The core of the system is the multi-channel neurostimulator SoC, first described in [15], that receives and amplifies EEG/ECoG signals from a microelectrode array implanted in the rodent brain. The amplified signals are filtered and digitized in each channel and then fed to an on-chip multi-core digital processor shared among channels, to extract their amplitude and phase information. The digital processor uses this information, as well as phase synchronization between different channels to detect an upcoming epileptic seizure and activate a subset of 24 current-mode stimulators available on the chip to abort it. The chip is interfaced with an on-board FPGA (Actel AGL060V5) that serializes the chip output and sends it to the wireless communication board through a vertical connector bus. The FPGA uses the same bus to receive configuration commands from the wireless board.

The wireless interface board receives and modulates data from the neurostimulator board and transmits it using an on-board low-power FSK (Frequency Shift Keying) transmitter. It also receives inductively-transmitted energy signals from the receiver coil that is connected to it, rectifies them and generates DC supply and bias voltages for different blocks on both boards (three low dropout regulators shown in Fig. 4). An ASK receiver is also placed on this board to receive commands that are sent through the inductive link. Both boards share a crystal oscillator output as their global operating clock.

B. Rodent Headset

Fig. 4(b) shows the miniaturized headset microsystem that is comprised of the two printed circuit boards (PCBs) and the receiver coil (on a flexible substrate) powered by an inductive powering rodent cage floor. The inductive floor which was

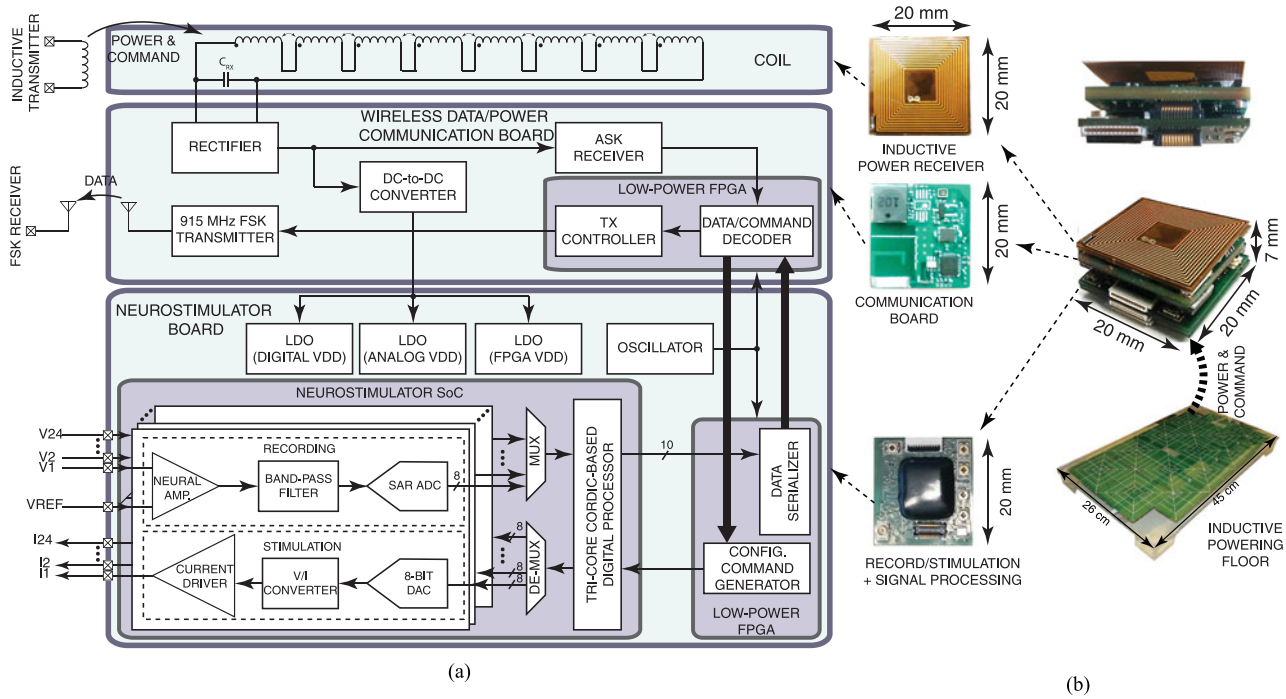

Fig. 4. (a) Simplified block diagram of the implantable inductively-powered closed-loop neurostimulator, (b) various components of the multi-PCB microsystem.

first reported in [75], is comprised of two overlapped arrays of 2×4 coils and sits under the animal cage. As illustrated, the power-receiving board (top) is a polyimide-based flexible coil that receives the power transmitted by means of near-field magnetic induction. It is connected to the wireless interface board (middle) that performs power management and supplies energy to different blocks of the system. In addition, this board hosts an FSK wireless transmitter to communicate recorded data to the outside of the body. The neurostimulator board (bottom) has the SoC [15] directly wire-bonded on it and covered by epoxy. It performs multi-channel signal recording and digital signal processing for monitoring and detection of epileptic seizures. The chip also does automatic multi-channel responsive electrical stimulation for seizure abortion.

C. Closed-loop Neurostimulator Board

Fig. 5(a) shows the top view of the neurostimulator board with the silicon SoC, shown in Fig. 5(d), directly bond-wired to it as depicted in Fig. 5(c). Fig. 5(b) shows the bottom view of the neural interface board. As shown, the board hosts the neurostimulator chip (bonded on top layer) as well as a low-power FPGA (soldered to bottom layer) that serializes and sends recorded neural data to the wireless interface board and controls the SoC mode of operation using commands received from that board. Microelectrode or ECoG arrays used for in vivo experiments connect to two 12-channel connectors on this board using flat flexible cables. Vertical Panasonic connectors are used to connect this board to the wireless interface board on one side, and to additional replicas of the neurostimulator board on the other side. Due to the direct wire-bonding constraints, only 24 channels of each SoC are used. For more channel count, more copies of the neurostimulator board are stacked vertically, each adding 24 to the total number of channels.

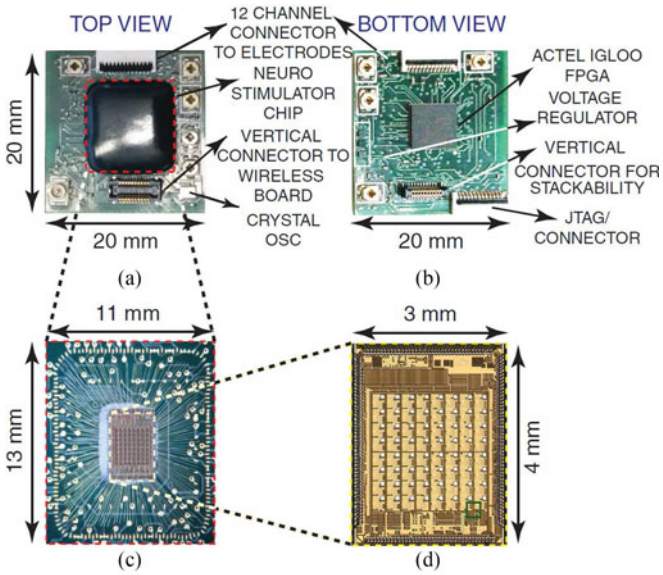

Fig. 5. (a) Top and (b) bottom views of the neurostimulator SoC wire-bonded to the neural interface PCB. (c) Two-tier bond wires under the epoxy cap. (d) A micrograph of the neurostimulator SoC, first presented in [15].

A synchrony-based on-chip processor [76] is integrated into the neurostimulator SoC [15] to conduct early epilepsy seizure detection. The processor is coupled with a set of 16/32-tap FIR filters that perform different filtering and averaging functions. For any selected pair of channels, first, two quadrature copies (i.e., 90 degrees phase shift) are generated using on-chip all-pass and Hilbert FIR filters [77]. The first core of the CORDIC processor uses these quadrature copies to calculate the phase for each signal as well as its magnitude. The second core gets the difference between the two calculated phases ($\Delta\phi$) as the input,

and computes $\sin(\Delta\phi)$ and $\cos(\Delta\phi)$. The on-chip FIR filters that were originally used to form all-pass and Hilbert filters are reprogrammed to take the moving average of the second core's outputs (i.e., $1/\mathrm{N} \times \Sigma\sin(\Delta\phi)$ and $1/\mathrm{N} \times \Sigma\sin(\Delta\phi)$) and feed it to the third core, where the phase locking value (PLV) is calculated as defined in [76].

In addition to the PLV, the magnitude and phase of each channel as well as the phase difference can be selected (using a multiplexer) as the output of the processor. A total of 54 clock cycles are required for the CORDIC processor (18 cycles per core) to compute the PLV algorithm. The processor contains 41,366 gates and occupies an area of 0.178 mm^2. The first core occupies 20.6 percent of the area, the second core uses 12.8 percent, the FIR moving-average filters occupy 57 percent, the third magnitude CORDIC core utilizes 9 percent and pre-processing and the output MUX occupy 1 percent of the total core area.

The on-chip processor is designed to operate autonomously to enable unsupervised closed-loop neurostimulation as a treatment alternative for patients with epilepsy. However, a number of parameters are reconfigurable on demand. This includes the processor's output (signal magnitude, phase, phase difference, or PLV), the threshold value for the output PLV that sets the border between seizure and non-seizure activity, and the processing delay set by the clock frequency. These parameters are set by the digital controller implemented in the on-board FPGA.

D. Digital Control

The communication between the wireless interface board and the neurostimulator board is controlled by 3 pins that are shared between them. The FPGA on the Neurostimulator board, reads the digitized brain recordings from the output of on-chip ADCs or the on-chip signal processing unit. The recorded brain data is then sent to the transmitter board as serial bits. Upon receiving each byte, the transmitter board sends it to a USB dongle through an SPI (Serial Peripheral Interface) bus. Due to the bandwidth limitations of the wireless transmitter, transmission of each byte takes more than 8 clock cycles. Only 20% of the transmit cycle is dedicated to data bits, and the rest is used for radio configuration. To avoid data loss and to maintain the synchrony between the two boards, every byte is followed by a certain number of zero bits to give the transmitter enough time to send a sample before the new one comes in. The minimum number of these zero bits is calculated depending on the maximum bandwidth of the transmitter and the frequency of the shared clock.

E. Data Communication and Power Management Board

Fig. 6(a) and (b) show the top and bottom views of the communication board with various discrete components such as the low-power FPGA, super capacitor, low dropout regulators, FSK transmitter, step-down converter, antenna, and different connectors attached to it. The FPGA receives the recorded neural signals from neurostimulator board, reformat the data, and sends it to the wireless FSK transmitter (TI CC1101). It also receives the output of the on-board ASK receiver, and decodes the configuration commands that are sent to the implant

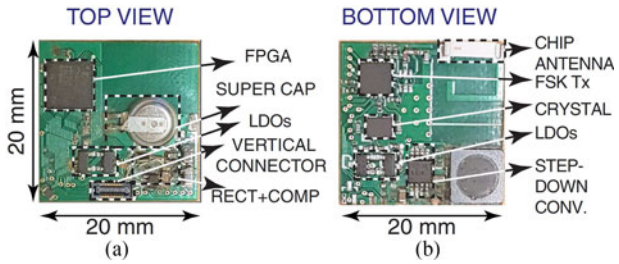

Fig. 6. (a) Top and (b) bottom views of the data communication and power management mini-PCB with various components annotated.

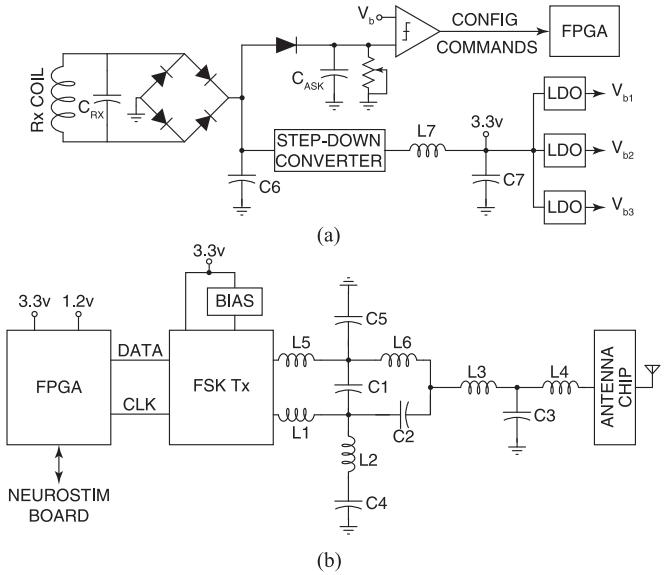

Fig. 7. Circuit schematic of the (a) inductive power reception and (b) FSK data transmission implemented on the communication board.

through the magnetic inductive link. Decoded commands are sent to the FPGA on the neurostimulator board to be applied to the chip.

Fig. 7 shows the simplified circuit schematic of the inductive power reception and wireless data transmission circuits as implemented on the communication board. As shown in Fig. 7(a), the power signals at the receiver are rectified, regulated, and fed to different LDOs to generate various supply and bias voltages. The rectified waveforms are also fed to an on-board ASK receiver to decode the ASK-modulated commands sent through the inductive link. The received commands are sent to the on-board FPGA, which is in communication with another FPGA on the neurostimulator board. Fig. 7(b) shows the simplified block diagram of wireless data transmission circuit. Through a vertical connector that attaches the two boards, the digitized neural data is sent from the neurostimulator board to the FPGA on the communication board. The data is then reorganized and sent to the on-board FSK transmitter which is connected to a planar on-board antenna.

Table IV lists all the discrete components used in both neurostimulator board and the communication board. Table V shows the value of passive elements used in the schematic depicted in Fig. 7.

TABLE IV
COMPONENTS USED IN THE BOARDS SHOWN IN FIGS. 5 AND 6

Neurostimulator Board		
Components	Company	Model
FPGA	ACTEL	AGL060V5
Regulators	Analog Devices	ADP121
Connector	Molex	5034801200
Vertical connector	Panasonic	AXT420324
		AXT420124
Trimmer	Murata	PVZ2
Crystal oscillator	Abracon	ASA 2–40 MHZ
Communication Board		
Components	Company	Model
FPGA	ACTEL	AGL060V5
LDO	Intersil	ISL60002
Vertical connector	Panasonic	AXT420124
Rectifier diodes	Broadcom	HSMP-389C
Buck converter	TI	TPS54062
FSK transmitter	TI	CC1101
Crystal	TI	NX3225GA
Inductor	Wurth Electronics	744062102
Chip Antenna	Johanson Tech.	0915AT43A0026E
Super Capacitor	Panasonic	EEC – EN0F204J1

TABLE V
PASSIVE ELEMENTS USED FOR THE CIRCUITS SHOWN IN FIG. 7

Components	Value	Components	Value
C1	1.25 pF	L1	12 nH
C2	1.75 pF	L2	18 nH
C3	3.5 pF	L3	12 nH
C4	100 pF	L4	12 nH
C5	1.5 pF	L5	12 nH
C6	1 μF	L6	18 nH
C7	200 mF	L7	1 mH

V. MEASUREMENT RESULTS

A. Experimental Characterization

Fig. 8 (top) shows the amplitude response of the front-end amplifier from sub-Hz frequencies up to the MHz range. The amplifier nominally operates between 0.5 Hz to 10 kHz, and its mid-band gain is measured to be over 53 dB for all of the channels. The experimentally measured CMRR (Common-Mode Rejection Ratio) at 10 Hz and 1 kHz is 75.4 dB and 71.5 dB, respectively. Both the high-pass and low-pass poles are adjustable, with the maximum bandwidth of 0.01 Hz to 10 kHz. Fig. 8(bottom) shows the integrated input-referred noise, which is measured to be 4.7 μV_{rms} when integrated from 10 Hz to 5 kHz, and 3.7 μV_{rms} for 1 Hz to 100 Hz. The noise efficiency factor is measured to be 4.4 for the 5 kHz bandwidth. Fig. 9 shows the frequency spectrum of the FSK wireless transmitter on the communication board that operates at 915 MHz, as well as an example of transmitted and received FSK-modulated data.

For freely moving rodent epilepsy studies, the implantable system is powered inductively. The powering system consists of a two-layer network of 16 planar high-Q (Q = 129) inductive transmitter coils placed under a non-conductive rat cage floor, and a small multi-layer flexible receiver coil, both shown in Fig. 4(b). The voltage received by the receiver coil is rectified and multiple on-board LDOs (Low DropOut regulator) are utilized to generate different supply and bias voltages required for the SoC and external components on both boards. The receiver coil is a 20 mm × 20 mm stack of several flexible two-layer PCBs. The flexibility allows to tailor-fit the coil to the shape of the implantation site.

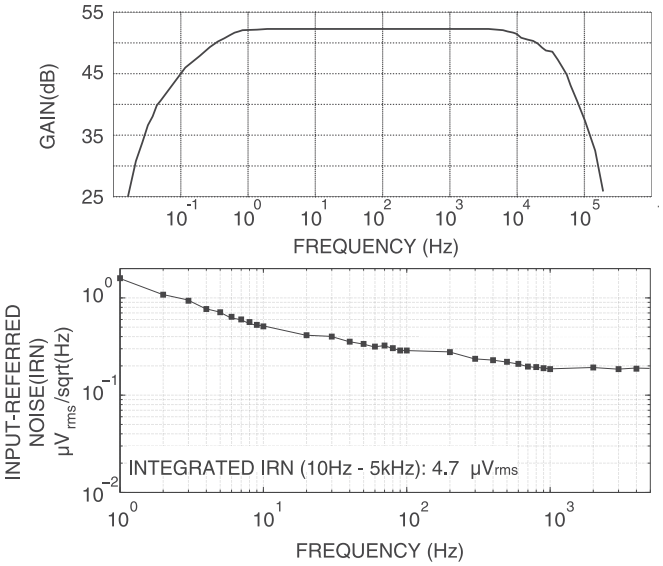

Fig. 8. Experimentally-measured frequency spectrum of the recording front-end (top), the input-referred noise (middle), and spectrum of the FSK transmitter (bottom).

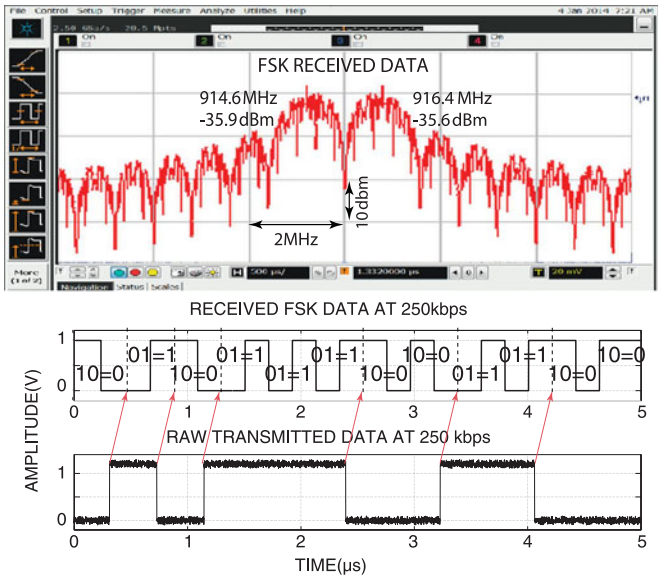

Fig. 9. Experimentally-measured (a) spectrum of the FSK transmitter, and (b) an example of transmitted and received FSK-modulated data.

B. Resource Utilization

The SoC operating in the recording mode dissipates 1.3 mW for all of the channels when running the FIR filters at 7.2 kS/s from a 1.2 V supply. The analog feed-forward path (including biasing) from the LNA to the output of the ADCs dissipates 886 μW. The digital adders and registers for the FIR filters, digital controller and the CORDIC processor dissipate 400μW. The neural stimulator (not included in Fig. 10) dissipates

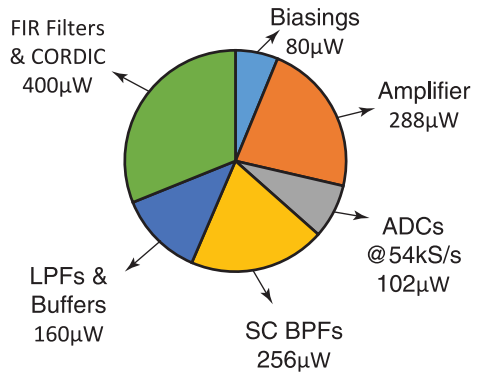

Fig. 10. Power breakdown of the neurostimulator SoC [15].

1.5 mW from a 3.3 V supply. This includes the DAC, control logic, V-to-I converter and output current driver operating with a 1 kHz 50 μA bi-phasic current at minimum duty cycle. The neural stimulator is not expected to be active during routine operation of the SoC and thus its power dissipation is not as critical when compared with the recording and signal processing functionalities.

Power dissipation can be reduced from 21.6 μW to 18 μW per channel by operating the digital FIR adder-and-delay logic and the CORDIC processor from a lower 0.8 V supply at the expense of requiring another voltage regulator. The neural stimulator can operate at a lower supply voltage (2.5 V) to further minimize power dissipation at the expense of voltage compliance.

VI. In Vivo Validation

A. Statistically-Significant: Using Software Processor of Early Seizure Detection and Control

Prior to validating the on-chip processor, a software-based version of it was ran on a computer. The computer received brain signals from the multi-channel neural front-end, and triggered electrical stimulators on the device upon the detection of an upcoming seizure. This way, the same recording and stimulation circuitry were used, but the processing was done in a computer. The experiment was done on several animals in both acute and chronic models of epilepsy in rats, and the detailed results of this algorithm-validating experiment is published in our previous work [73]. A total of 598 seizures (494 chronic model, and 104 acute model) were recorded. For the chronic model the algorithm could detect 88% of the seizures with a 0.67 false positives per day. Once the feedback stimulation was turned on, seizure occurrence frequency was reduced by 80% to 100% for different animals.

As shown in Fig. 11, the seizure occurrence frequency was measured for 4 periods, each lasting 7 days: (a) no stimulation, (b) closed-loop stimulation, (c) no stimulation, and (d) open-loop stimulation. This scenario is chosen as it clearly shows the effectiveness of closed-loop stimulation as well as its performance compared to open-loop stimulation.

B. Proof-of-Concept: Using On-chip Processor

The SoC was validated (using a larger bench-top test PCB board [15]) in an in vivo experiment using a rodent model of

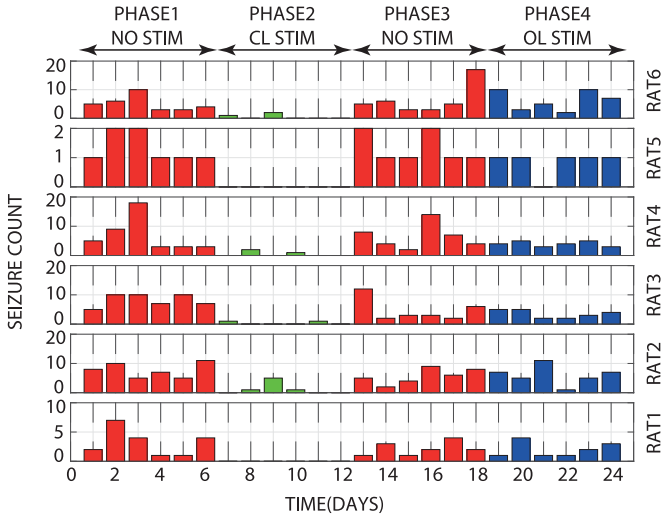

Fig. 11. Seizure suppression results in the four-phase chronic experiment.

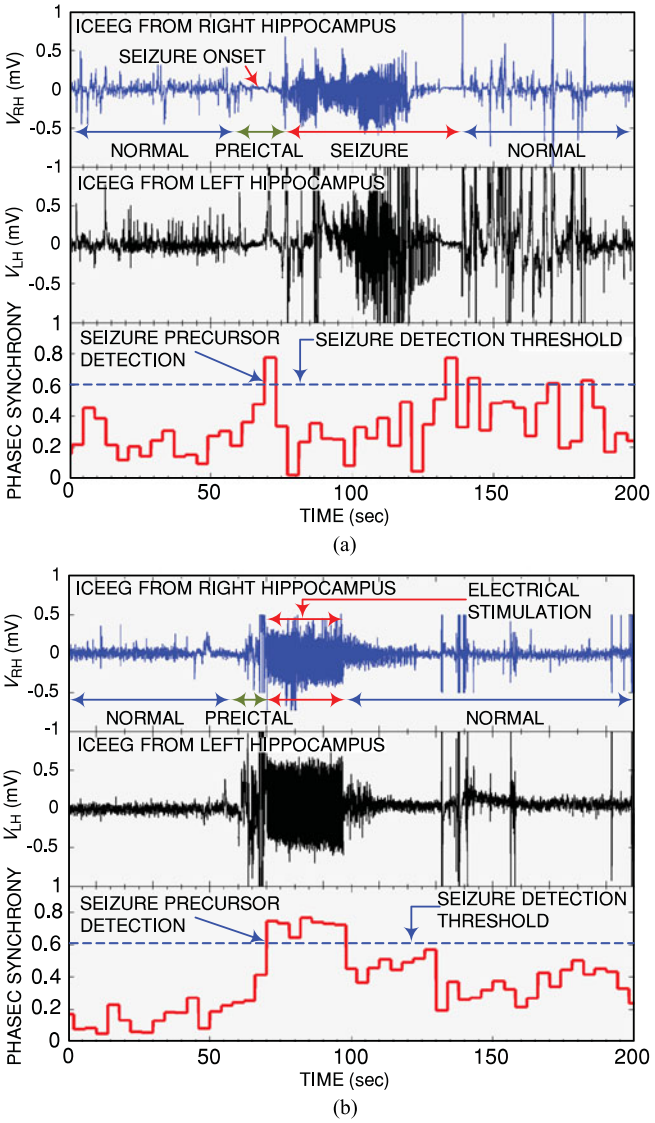

Fig. 12. Experimentally measured results: (a) an example of an early seizure detection in the non-treatment group, and (b) an example of a seizure abortion in the treatment group of rats.

TABLE VI
STATE-OF-THE-ART MINIATURIZED NEURAL RECORDING AND/OR STIMULATION SOC-BASED SYSTEMS

Specifications	[11] TBIOCAS 2011 Mohseni	[8] TBIOCAS 2010 Meng	[9] TBIOCAS 2013 Genov	[21] JSSC 2015 Rabaey	[12] TBIOCAS 2015 Chen	THIS WORK
Targeted Application	Intracortical Microstimulation	Neural Monitoring	Rat ECoG Rec. & stim.	Neural Monitoring	Closed-loop Neurostimulation	Epileptic Seizure Detection and Control
Size (cm^3)	$3.6 \times 1.3 \times 0.6$	$3.8 \times 3.8 \times 5.1$	$3 \times 2.2 \times 1.5$	N/R	$3 \times 2.5 \times 2.5$*	$2 \times 2 \times 0.7$
Weight (gr)	1.7	N/R	12	–	20	6
Number of Rec. Channels	4	32	256	64	8	24
SIGNAL PROCESSING	YES	NO	NO	NO	YES	YES
Closed-loop Detection	YES	–	–	NO	YES	YES
Method	Spike-Discriminator	–	–	–	Phase & Magnitude	Phase Synchrony
NEURAL STIMULATION	YES	NO	YES	NO	YES	YES
# of Stim. Channels	4	0	64	0	8	24
Current Range	125 μA	–	20–250 μA	–	82.5–229 μA	10 μA–1 mA
ENERGY SOURCE	Battery	Battery	Battery	Magnetic Induction	Magnetic Induction	Magnetic Induction
Battery Lifetime (hr)	24	33	10	–	–	–
Receiver Coil Type	–	–	–	1-layer flex	1-layer flex	multi-layer flex
Coil Separation	–	–	–	1.6 cm	6 mm	$<$15 cm
WIRELESS COMM.	YES	YES	YES	YES	YES	YES
Modulation	FSK	FSK	ZigBee	OOK	ASK	FSK
Frequency	433 MHz	3.9 GHz	2.4 GHz	300 MHz	10 MHz	915 MHz
Max. Range	1m	$>$ 20 m	N/R	N/R	6 mm	10 m
IN-VIVO RESULTS	YES	YES	YES	YES	YES	YES
Sensitivity (%)	–	–	–	–	–	88–96
Selectivity (%)	–	–	–	–	–	89–97

*: Estimated, -: Not Applicable, N/R: Not Reported

epilepsy. Four Wistar rats were intraperitoneally injected with kainic acid which induced recurrent spontaneous motor seizures within one to two months. The rats underwent craniotomy for both hippocampi and frontal lobe microelectrodes implantation. The rats were divided into two equal groups: the non-stimulation group and the stimulation group. In each rat, the electrodes were connected to the presented SoC for automatic seizure detection. Each rat was also video monitored for seizure labeling. Fig. 12 (a) shows an example of in-vivo real-time seizure detection in the non-stimulation group.

In the stimulation group the SoC was also configured to trigger the closed-loop electrical stimulation in response to a seizure onset detection. Fig. 12(b) illustrates the SoC-triggered stimulation upon a seizure onset detection in the stimulation group and the seizure having been suppressed.

The average sensitivity and specificity of the detection were 87% and 95%, respectively. Seizure frequency has been reduced on average by over 76% in the stimulation group compared to the non-stimulation group.

In a second implementation, a four times complex signal processing algorithm was deployed on a stationary device. This requires a 200 kbps wireless data communication forward link. As a result, the detection performance was improved to a sensitivity of 98% with three times fewer false alarms, in cost of additional power for in-implant wireless transmitter.

A comparative analysis is given in Table VI where this work demonstrates advanced functionality among recently published state-of-the-art miniaturized SoC-based neural interfaces. The main difference between the works cited in this table compared to the previous one is that Table III compares brain interface SoCs with an integrated DSP for a neurological event detection, while Table VI includes devices of similar nature, but only those that are miniaturized for implantation.

VII. COMMUNICATION AND COMPUTATION TRADEOFF

One of the key design considerations for implantable neurostimulators is the power-tradeoff between wireless communication and on-chip signal processing. This is discussed in details in our previous work [74]. In this design, the experimentally-measured power consumption of the on-chip processor is 897 μW for a clock frequency of 10 MHz and supply voltage of 1.15 V. To reduce power consumption, both supply voltage and clock frequency could be reduced to 0.85 V and 2.5 MHz, respectively, at the cost of a higher detection latency. For a 1.15 V supply at 2.5 MHz the processor dissipates 231 μW, and for a 0.85 V supply at 2.5 MHz and 10 MHz the processor dissipates 102 μW and 412μW, respectively.

Based on these power figures, the seizure detector processor dissipates 3.6 μW/channel and has an energy efficiency of 210 pJ/bit. If the processing is to be performed off-chip, the raw recorded data must be transmitted, and the stimulation commands must be received wirelessly to and from a computer base station, respectively, which translates to an energy efficiency of 3.37 nJ/bit.

Based on the above, although performing seizure detection on a computer results in slightly higher accuracy (5%), it results

is degrading the energy efficiency by a factor of 16, and a higher latency in seizure detection.

VIII. Conclusion

A neurostimulator with high treatment efficacy has been sought after for a long time. In this work, first we presented commercially-available open-loop and closed-loop neurostimulators, and showed that their low treatment efficacy is rooted from absence or poor performance of their brain monitoring (signal processing) feature. As a natural next step, we reviewed signal processing algorithms and evaluated them in terms of accuracy, latency, and feasibility for hardware implementation in an implantable device. The review's focus is on algorithms designed for early detection of epilepsy seizures, and its goal is to find the optimum signal features and classification method to accomplish highest-possible detection accuracy. The review reveals that high-cost approaches such as increasing the number of temporal, spatial, or spectral features, and implementing a very advanced machine-learning-based classifier are not as rewarding as selecting and combining the right patient-specific features. Once the right features are selected, a simple thresholding could yield a highly-accurate, yet low-cost classifier.

Having the review conclusions taken into account, a phase-synchrony based detection algorithm is selected, and integrated into a 24-channel wireless and battery-less implantable microsystem as a design example. The system records neural signals at high spatial resolution, processes them on-chip to predict epileptic seizures and performs multi-channel responsive current-mode electrical stimulation upon a prediction. A wireless transmitter communicates recorded neural activity as well as signal processing results to a remote computer. Energy is provided to the system using magnetic induction. Small form factor, light weight, lack of wires and autonomous operation make the system excellent for chronic implantation. The approach was fully characterized electronically and was validated on freely moving animals with temporal lobe epilepsy, both with a computer model of the system connected in the stimulation loop and with the neurostimulator SoC in the loop.

References

[1] "Neurological disorders: Public health challenges," World Health Organization, Geneva, Switzerland, 2006.

[2] S. S. Spencer, D. K. Nguyen, and R. B. Duckrow, "Invasive EEG in presurgical evaluation of epilepsy," *Treatment Epilepsy*, vol. 4, pp. 767–798, 2009.

[3] H. S. Mayberg *et al.*, "Deep brain stimulation for treatment-resistant depression," *Neuron*, vol. 45, no. 5, pp. 651–660, 2005.

[4] M. C. Rodriguez-Oroz *et al.*, "Bilateral deep brain stimulation in Parkinson's disease: A multicentre study with 4 years follow-up," *Brain*, vol. 128, no. 10, 2240–2249, 2005.

[5] F. Mormann, R. G. Andrzejak, C. E. Elger, and K. Lenhnertz, "Seizure prediction: The long and the winding road," *Brain*, vol. 130, no. 2, pp. 314–33, 2007.

[6] D. Snyder and K. W. Leyde, "Methods and systems for characterizing and generating a patient-specific seizure advisory system," U.S. Patent Application 12/035,335, filed Feb. 21, 2008.

[7] J. Cook *et al.*, "Prediction of seizure likelihood with a long-term, implanted seizure advisory system in patients with drug-resistant epilepsy: A first-in-man study," *The Lancet Neuro.*, vol. 12, No. 6, pp. 563–571, Jun. 2013.

[8] H. Miranda, V. Gilja, C. Chestek, K. Shenoy, and T. Meng, "HermesD: A high-rate long-range wireless transmission system for simultaneous multichannel neural recording applications," *IEEE Trans. Biomed. Circuits Syst.*, vol. 4, no. 3, pp. 181–191, Jun. 2010.

[9] A. Bagheri *et al.*, "Massively-parallel neuromonitoring and neurostimulation rodent headset with nanotextured flexible microelectrodes," *IEEE Trans. Biomed. Circuits Syst.*, vol. 7, no. 5, pp. 601–609, Oct. 2013.

[10] F. T. Sun, M. Morrell, and R. Wharen, "Responsive cortical stimulation for the treatment of epilepsy," *Neurotherapeutics*, vol. 5, pp. 68–74, 2008.

[11] M. Azin, D. Guggenmos, S. Barbay, R. Nudo, and P. Mohseni, "A miniaturized system for spike-triggered intracortical microstimulation in an ambulatory rat," *IEEE Trans. Biomed. Eng.*, vol. 58, no. 9, pp. 2589–2597, Sep. 2011.

[12] Y.-P. Lin *et al.*, "A battery-less, implantable neuro-electronic interface for studying the mechanisms of deep brain stimulation in rat models," *IEEE Trans. Biomed. Circuits Syst.*, vol. 10, no. 1, pp. 98–112, Feb. 2016.

[13] H. Kassiri, G. Dutta, N. Soltani, C. Liu, Y. Hu, and R. Genov, "An impedance-tracking battery-less arbitrary-waveform neurostimulator with load-adaptive 20V voltage compliance," in *Proc. IEEE Eur. Solid-State Circuits Conf.*, Sep. 2016, pp. 225–228.

[14] H. Kassiri *et al.*, "All-wireless 64-channel 0.013mm2/ch closed-loop neurostimulator with rail-to-rail DC offset removal," in *Proc. IEEE Int. Solid-State Circuits Conf.*, Feb. 2017, pp. 452–453.

[15] K. Abdelhalim, H. Jafari, L. Kokarovtseva, J. L. Perez Velazquez, and R. Genov, "64-channel UWB wireless neural vector analyzer SOC with a closed-loop phase synchrony-triggered neurostimulator," *IEEE J. Solid-State Circuits*, vol. 48, no. 10, pp. 2494–2510, Oct. 2013.

[16] R. Harrison *et al.*, "A low-power integrated circuit for a wireless 100-electrode neural recording system," *IEEE J. Solid State Circuits*, vol. 42, no. 1, pp. 123–133, Jan. 2007.

[17] S. Zanos, A. Richardson, L. Shupe, and E. Fetz, "The neurochip-2: An autonomous head-fixed computer for recording and stimulating in freely behaving monkeys," *IEEE Trans. Neural Syst. Rehabil. Eng.*, vol. 19, no. 4, pp. 427–435, Aug. 2011.

[18] N. Soltani, H. Kassiri, H. Jafari, K. Abdelhalim, and R. Genov, "130 nm CMOS 230Mbps 21pJ/b UWB-IR transmitter with 21.3% efficiency," in *Proc. IEEE Eur. Solid-State Circuits Conf.*, 2015, pp. 352–355.

[19] C. P. Young, S. Liang, D. Chang, Y. Liao, F. Shaw, and C. Hsieh, "A portable wireless online closed-loop seizure controller in freely moving rats," *IEEE Trans. Instrum. Meas.*, vol. 60, no. 2, pp. 513–521, Feb. 2011.

[20] H. Kassiri *et al.*, "Inductively-powered direct-coupled 64-channel chopper-stabilized epilepsy-responsive neurostimulator with digital offset cancellation and Tri-band radio," in *Proc. IEEE Eur. Solid-State Circuits Conf.*, Venice, Italy, Sep. 2014, pp. 95–98.

[21] R. Muller *et al.*, "A minimally invasive 64–channel wireless μECoG implant," *IEEE J. Solid–State Circuits*, vol. 50, no. 1, pp. 344–359, Jan. 2015.

[22] J. A. Johnson, *FDA Regulation of Medical Devices*. Washington, DC, USA: Congressional Research Service, 2012.

[23] H. Kassiri *et al.*, "Inductively powered arbitrary-waveform adaptive-supply electro-optical neurostimulator," in *Proc. IEEE Biomed. Circuits Syst. Conf.*, Atlanta, GA, USA, Oct. 2015.

[24] A. Chemparathy *et al.*, "Wearable low-latency sleep stage classifier," in *Proc. IEEE Biomed. Circuits Syst. Conf.*, Lausanne, Switzerland, Oct. 2014, pp. 592–595.

[25] H. Kassiri *et al.*, "Battery-less Tri-band-radio neuro-monitor and responsive neuro-stimulator for diagnostics and treatment of neurological disorders," *IEEE J. Solid-State Circuits*, vol. 51, no. 5, pp. 1274–1289, May 2016.

[26] H. Kassiri, N. Soltani, M. T. Salam, R. Genov, and J. P. Velazquez, "Battery-less modular responsive neurostimulator for prediction and abortion of epileptic seizures," in *Proc. IEEE Int. Symp. Circuits Syst.* 2016, pp. 1298–1301.

[27] G. L. Morris and W. M. Mueller, "Long-term treatment with vagus nerve stimulation in patients with refractory epilepsy," *Neurology*, vol. 53, p. 1731, 1999.

[28] P. Boggiob *et al.*, "Effects of transcranial direct current stimulation on working memory in patients with Parkinson's disease." *J. Neuro. Sci.*, vol. 249, no. 1, pp. 31–38, 2006.

[29] "Vercise PC DBS system," Boston Scientific, Marlborough, MA, USA. 2015. [Online]. Available: http://www.bostonscientific.com/en-EU/products/deep-brain-stimulation-systems/Vercise-PC-DBS.html

[30] "Boston scientific device exhibit," Boston Scientific, Marlborough, MA, USA. 2015. [Online]. Available: http://braininitiative.nih.gov/pdf/ BostonScientificDeviceExhibits092015_508C.pdf

[31] U. Springer, D. Bowers, W. Goodman, N. Shapira, K. Foote, and M. Okun, "Long-term habituation of the smile response with deep brain stimulation," *Neurocase*, vol. 12, no. 3, pp. 191–196, 2006.

[32] "Activa RC multi-program rechargable neurostimulator," Medtronic, Minneapolis, MN, USA. 2009. [Online]. Available: http://manuals.medtronic.com/wcm/groups/mdtcom_sg/@emanuals

[33] "Constant current for constant symptom control," St. Jude Medical, Saint Paul, MN, USA. 2013. [Online]. Available: http://www.deltamedicalbrasilia.com.br/wp-content/uploads/2011/09/catalogo-dbs.pdf

[34] "Brio deep brain stimulation rechargeable implant pulse generator," St. Jude Medical, Saint Paul, MN, USA. 2011. [Online]. Available: http://www.cardion.cz/file/189/brio-specsheet.pdf

[35] "Cyberonics images and captions," Cyberonics, Houston, TX, USA. 2013. [Online]. Available: https://www.cyberonics.com/download/135

[36] "New medtronic deep brain stimulation system the first to sense and record brain activity while delivering therapy," Medtronic, Dublin, Ireland. 2013. [Online]. Available: http://newsroom.medtronic.com/phoenix.zhtml?c=251324&p=irol-newsArticle

[37] "RNS system user manual," NeuroPace, Mountain View, CA, USA. 2015. [Online]. Available: http://www.neuropace.com/product/pdfs/RNS_System_User_Manual.pdf

[38] "The RNS system, targeted treatment when its needed," *NeuroPace*, Mountain View, CA, USA. 2015. [Online]. Available: http://www.neuropace.com/product/overview.html

[39] C. Deckers, P. Genton, G. Sills, and D. Schmidt, "Current limitations of antiepileptic drugtherapy: A conference review," *Epilepsy Res.*, vol. 53, pp. 1–17, 2003.

[40] M. Winterhalder, T. Maiwald, H. Voss, R. Aschenbrenner-Scheibe, K. Timmer, and A. Schulze-Bonhage, "The seizure prediction characteristic: A general framework to assessand compare seizure prediction methods," *Epilepsy Behav.*, vol. 4, pp. 318–25, 2003.

[41] R. Aschenbrenner-Scheibe, T. Maiwald, M. Winterhalder, H. Voss, J. Timmer, and A. Schulze-Bonhage, "How well can epileptic seizures be predicted? An evaluation of anonlinear method," *Brain*, vol. 126, pp. 2616–26, 2003.

[42] F. Mormann, R. G. Andrzejak, C. E. Elger, and K. Lehnertz, "Seizure prediction: The long and winding road," *J. Neurol., Brain*, vol. 130, no. 2, pp. 314–333, Sep. 2007.

[43] N. C. Bhavaraju, M. G. Frei, and I. Osorio, "Analog seizure detection and performance evaluation," *IEEE Trans. Biomed. Eng.*, vol. 53, no. 2, pp. 238–245, Feb. 2006.

[44] B. Litt *et al.*, "Epileptic seizures may begin hours in advance of clinical onset: A report of five patients," *J. Neuron*, vol. 30, no. 1, pp. 51–64, Apr. 2001.

[45] C. Elger and K. Lehnertz, "Seizure prediction by non-linear time series analysis of brain electrical activity," *Eur. J. Neurosci.*, vol. 10, pp. 786–789, Oct. 1998.

[46] L. Iasemidis *et al.*, "Adaptive epileptic seizure prediction system," *IEEE Trans. Biomed. Eng.*, vol. 50, no. 5, pp. 616–627, May 2003.

[47] F. Mormann, K. Lehnertza, P. Davidb, and C. E. Elgera, "Mean phase coherence as a measure for phase synchronization and its application to the EEG of epilepsy patients," *J. Phys. D, Nonlinear Phenom.*, vol. 144, no. 1, pp. 358–369, Oct. 2000.

[48] T. I. Netoff and S. J. Schiff, "Decreased neuronal synchronization during experimental seizures," *J. Neurosci.*, vol. 22, no. 16, pp. 7297–7307, Aug. 2002.

[49] P. Mirowski, D. Madhavan, Y. LeCun, and R. Kuzniecky, "Classification of patterns of EEG synchronization for seizure prediction," *J. Clin. Neurophysiol.*, vol. 120, pp. 1927–1940, Oct. 2009.

[50] D. Gupta and C. J. James, "Narrowband vs. broadband phase synchronization analysis applied to independent components of ictal and interictal EEG," in *Proc. Annu. Int. Conf. IEEE Eng. Med. Biol. Soc.*, 2007, pp. 3864–3867.

[51] B. Schelter *et al.*, "Testing statistical significance of multivariate time series analysis techniques for epileptic seizure prediction," *CHAOS Amer. Inst. Phys.*, vol. 16, pp. 1–10, Jan. 2006.

[52] T. Maiwald, M. Winterhalder, R. Aschenbrenner-Scheibe, H. U. Voss, A. Schulze-Bonhage, and J. Timmer, "Comparison of three nonlinear seizure prediction methods by means of the seizure prediction characteristic," *Physica D*, vol. 194, no. 3/4, pp. 357–368, Jul. 2004.

[53] F. Mormann, R. G. Andrzejak, C. E. Elger, and K. Lehnertz, "Seizure prediction: The long and winding road," *Brain*, vol. 130, pp. 314–333, Sep. 2007.

[54] R. Harrison *et al.*, "Wireless neural recording with single low-power integrated circuit," *IEEE Trans. Neural Syst. Rehabil. Eng.*, vol. 17, no. 4, pp. 322–329, Aug. 2009.

[55] J. R. Williamson, D. W. Bliss, D. Browne, and J. Narayanan, "Seizure prediction using EEG spatiotemporal correlation structure," *Epilepsy Behav.*, vol. 25, pp. 230–238, 2012.

[56] S. Li, W. Zhou, Q. Yuan, and Y. Liu, "Seizure prediction using spike rate of intracranial EEG," *IEEE Trans. Neural Syst. Rehabil. Eng.*, vol. 21, no. 6, pp. 880–886, Nov. 2013.

[57] A. Eftekhar, W. Juffali, J. El-Imad, T. Constandinou, and C. Toumazou, "Ngram-derived pat-tern recognition for the detection and prediction of epileptic seizures," *PLoS One*, vol. 9, 2014, Art. no. e96235.

[58] Y. Zheng, G. Wang, K. Li, G. Bao, and J. Wang, "Epileptic seizure prediction using phasesynchronization based on bivariate empirical mode decomposition," *Clin. Neurophysiol.*, vol. 125, pp. 1104–1111, 2014.

[59] L. Kuhlmann *et al.*, "Patient-specific bivariate-synchrony-based seizure prediction for short predictionhorizons," *Epilepsy Res.*, vol. 91, pp. 214–231, 2010.

[60] B. Schelter *et al.*, "Testing statistical significance of multivariate time series analysis techniquesfor epileptic seizure prediction," *Chaos*, vol. 16, 2006, Art. no. 013108.

[61] Y. Park, L. Luo, K. Parhi, and T. Netoff, "Seizure prediction with spectral power of EEG usingcost-sensitive support vector machines," *Epilepsia*, vol. 52, pp. 1761–1770, 2011.

[62] K. Gadhoumi, J. Lina, and J. Gotman, "Seizure prediction in patients with mesial temporal lobe epilepsy using EEG measures of state similarity," *Clin. Neurophysiol.*, vol. 124, pp. 1745–1754, 2013.

[63] M. Bandarabadi, C. Teixeira, J. Rasekhi, and A. Dourado, "Epileptic seizure prediction usingrelative spectral power features," *Clin. Neurophysiol.*, vol. 126, no. 2, pp. 237–248, 2015.

[64] F. Mormann *et al.*, "On the pre-dictability of epileptic seizures," *Clin. Neurophysiol.*, vol. 116, pp 569–587, 2005.

[65] F. Mormann, T. Kreuz, R. G. Andrzejak, P. David, K. Lehnertz, and C. Elger, "Epileptic seizuresare preceded by a decrease in synchronization," *Epilepsy Res.*, vol. 53, pp. 173–185, 2003.

[66] A. Avestruz *et al.*, "A 5 μW/channel spectral analysis IC for chronic bidirectional brainmachine interfaces," *IEEE J. Solid-State Circuits*, vol. 43, no. 12, pp. 3006–3024, Dec. 2008.

[67] M. Chae, Z. Yang, M. R. Yuce, L. Hoang, and W. Liu, "A 128-channel 6 mW wireless neural recording IC with spike feature extraction and UWB transmitter," *IEEE Trans. Neural Syst. Rehabil. Eng.*, vol. 17, no. 4, pp. 312–321, Aug. 2009.

[68] T. Chen *et al.*, "1.4 μW/channel 16-channel EEG/ECoG processor for smart brain sensor SoC," in *Proc. IEEE Symp. VLSI Circuits*, Jun. 2010, pp. 21–22.

[69] N. Verma *et al.*, "A micro-power EEG acquisition SoC with integrated feature extraction processor for a chronic seizure detection system," *IEEE J. Solid-State Circuits*, vol. 45, no. 4, pp. 804–816, Apr. 2010.

[70] J. Yoo, L. Yan, D. E. Damak, M. A. B. Altaf, A. H. Shoeb, and A. P. Chandrakasan, "An 8-channel scalable EEG acquisition SoC with patient-specific seizure classification and recording processor," *IEEE J. Solid-State Circuits*, vol. 48, no. 1, pp. 214–228, Jan. 2013.

[71] W. M. Chen *et al.*, "A fully integrated 8-channel closed-loop neural-prosthetic CMOS SoC for real-time epileptic seizure control," *IEEE J. Solid-State Circuits*, vol. 49, no. 1, pp. 232–247, Jan. 2014.

[72] M. Shoaran, C. Pollo, K. Schindler, and A. Schmid, "A fully-integrated IC with 0.85 μW/Channel consumption for epileptic iEEG detection," *IEEE Trans. Circuits Sys. II, Express Briefs*, vol. 62, no. 2, pp. 114–118, Feb. 2015.

[73] M. T. Salam, H. Kassiri, R. Genov, and J. L. Perez Velazquez, "Rapid brief feedback intracerebral stimulation based on real-time desynchronization detection preceding seizures stops the generation of convulsive paroxysms," *Epilepsia*, vol. 56, no. 8, pp. 1227–1238, 2015.

[74] M. T. Salam, H. Kassiri, N. Soltani, H. He, J. L. Velazquez, and R. Genov, "Tradeoffs between wireless communication and computation in closed-loop implantable devices," in *Proc. IEEE Int. Symp. Circuits Syst.*, 2016, pp. 1838–1841.

[75] N. Soltani, M. S. Aliroteh, and R. Genov, "Cellular inductive powering system for weakly-linked resonant rodent implants," in *Proc. IEEE Biomed. Circuits Syst. Conf.*, Rotterdam, The Netherlands, Oct. 2013, pp. 350–353.

[76] K. Abdelhalim, V. Smolyakov, and R. Genov, "A phase-synchronization epileptic seizure detector VLSI architecture," *IEEE Trans. Biomed. Circuits Syst.*, vol. 5, no. 5, pp. 430–438, Oct. 2011.

[77] K. Abdelhalim, V. Smolyakov, and R. Genov, "Phase-synchronization early epileptic seizure detector VLSI architecture," *IEEE Trans. Biomed. Circuits Syst.*, vol. 5, no. 5, pp. 430–438, Oct. 2011.

[78] G. Sukhi and G. Jean, "An automatic warning system for epileptic seizures recorded on intracerebral EEGs," *Clin. Neurophysiol.*, vol. 116, pp. 2460–2472, 2005.

[79] L. Guo *et al.*, "Automatic epileptic seizure detection in EEGs based on line length feature and artifical neural networks," *J. Neurosci. Methods*, vol. 191, pp. 101–9, 2010.
[80] Q. Yuan *et al.*, "Epileptic EEG classification based on extreme learning machine and nonlinear features," *Epilepsy Res.*, vol. 96, no. 1, pp. 29–38, 2011.
[81] J. L. Perez Velazquez *et al.*, "Experimental observation of increased fluctuations in an order parameter before epochs of extended brain synchronization," *J. Biol. Phys.*, vol. 37, pp. 141–152, 2011.
[82] K. Polat and S. Gne, "Classification of epileptiform EEG using a hybrid system based on detection tree classifier and fast Fourier transform," *Appl. Math. Comput.*, vol. 186, no. 2, pp. 1017–1026, 2007.

Hossein Kassiri (S'10–M'16) received the B.Sc. degree from the University of Tehran, Tehran, Iran, in 2008, the M.A.Sc. degree from McMaster University, Hamilton, ON, Canada, in 2010, and the Ph.D. degree from the University of Toronto, Toronto, ON, Canada, in 2016, all in electrical and computer engineering. During the Ph.D. degree, he focused on the design, development, and validation of wireless and battery-less neural recording and stimulation systems and their application in monitoring and treatment of neurological disorders.

He is currently an Assistant Professor in the Department of Electrical Engineering and Computer Science, York University, Toronto, ON, Canada, where he is a member of Nanotechnology and Biotechnology Research Group and the Director of the Integrated Circuits and Systems Lab. He also holds the position of CTO at BrainCom Inc., a company he co-founded in September 2015, specialized in implantable brain-computer interfaces. He received the IEEE ISCAS best paper award (BioCAS track) in 2016, Ontario Brain Institute entrepreneurship award in 2015, Heffernan Commercialization award in 2014, and the CMC Brian L. Barge award for excellence in microsystems integration in 2012.

Sana Tonekaboni received the B.Sc. degree in electrical engineering from the University of Toronto, Toronto, ON, Canada, in 2017. As an Undergraduate Research Assistant, she was involved in different biomedical, bioinformatics, and signal processing research and received the NSERC USRA award in 2015 and 2016.

M. Tariqus Salam (M'09) received the B.Sc. degree in electrical and electronics engineering from Islamic University of Technology, Gazipur City, Bangladesh, in 2003, the M.A.Sc. degree in electrical and computer engineering from Concordia University, Montreal, QC, Canada, in 2007, and the Ph.D. degree in electrical engineering from Polytechnique Montréal, Montreal, QC, Canada, in 2012. From 2012 to 2015, he was a Postdoctoral Fellow at the University of Toronto, where he worked in the Neuroscience division of Toronto Western Hospital. He is currently with Galvani Bioelectronics as an R&D Electronic Engineer for neuromodulation devices. His main research interests include the areas of low-power circuit design, brain-machine interface, and mental disease diagnosis and therapy.

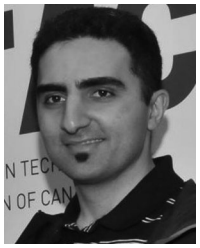

Nima Soltani received the B.Eng. and M.A.Sc. degrees from Ryerson University, Toronto, ON, USA, in 2007 and 2010, respectively, and the Ph.D. degree from the University of Toronto, Toronto, ON, Canada, in 2016, all in electrical engineering. From 2010 to 2011, he worked at the Solace Power Inc., on the development of the first electrical induction system for medium-range wireless power transfer. His Ph.D. thesis focused on inductively-powered implantable brain chemistry monitoring systems. He is a co-founder of the BrainCom Inc., and currently works as an analog/mixed-signal design engineer at Synopsys Inc.

Karim Abdelhalim received the B.Eng. and M.A.Sc. degrees in electrical engineering from Carleton University, Ottawa, ON, Canada, in 2005 and 2007, respectively, and the Ph.D. degree in 2013 in electrical and computer engineering from the University of Toronto, Toronto, ON, Canada, where he focused on wireless neural recording and stimulation SoCs and their application in monitoring and treatment of intractable epilepsy.

From 2011 to 2015, he was a Senior Staff Scientist at Broadcom Corporation, Irvine, CA, USA, where he was involved with the design of mixed-signal ICs for 10/100/1G-BASE-T Ethernet applications and 100BASE-T1 and 1000BASE-T1 automotive Ethernet applications. From July 2010 to October 2010, he also worked as a mixed-signal design engineering intern at Broadcom, Irvine, CA, USA. Since 2015, he has been a Senior Staff analog integrated circuit design engineer with Inphi Corporation, Irvine, CA, USA, where his main focus is ultra high-speed transceivers for optical applications.

Jose Luis Perez Velazquez was born in Zaragoza, Spain. He received the Licenciado degrees in chemistry from the University of Zaragoza, Aragon, Spain, and in biochemistry from Complutense University of Madrid, Madrid, Spain, and the Ph.D. degree from the Department of Molecular Physiology and Biophysics, Baylor College of Medicine, Houston, TX, USA, in 1992, and homologated to Doctorate degree in chemistry by the Spanish Ministry of Culture in 1997.

He is currently an Associate Scientist in the Neuroscience and Mental Programme and the Brain and Behaviour Center, Hospital For Sick Children, Toronto, ON, Canada, and an Associate Professor at the University of Toronto, Toronto, ON, Canada.

Roman Genov (S'96–M'02–SM'11) received the B.S. degree in electrical engineering from Rochester Institute of Technology, Rochester, NY, USA, in 1996, and the M.S.E. and Ph.D. degrees in electrical and computer engineering from Johns Hopkins University, Baltimore, MD, USA, in 1998 and 2003, respectively.

He is currently a Professor in the Department of Electrical and Computer Engineering, University of Toronto, Toronto, ON, Canada, where he is a member of Electronics Group and Biomedical Engineering Group and the Director of Intelligent Sensory Microsystems Laboratory. His research interests include primarily in analog integrated circuits and systems for energy-constrained biological, medical, and consumer sensory applications.

Dr. Genov is a co-recipient of Best Paper Award at the IEEE Biomedical Circuits and Systems Conference, Best Student Paper Award at the IEEE International Symposium on Circuits and Systems, Best Paper Award of the IEEE Circuits and Systems Society Sensory Systems Technical Committee, Brian L. Barge Award for Excellence in Microsystems Integration, MEMSCAP Microsystems Design Award, DALSA Corporation Award for Excellence in Microsystems Innovation, and Canadian Institutes of Health Research Next Generation Award. He was a Technical Program Co-Chair at the IEEE Biomedical Circuits and Systems Conference. He was an Associate Editor of the IEEE TRANSACTIONS ON CIRCUITS AND SYSTEMS-II: EXPRESS BRIEFS and the IEEE SIGNAL PROCESSING LETTERS, and a member of the IEEE International Solid-State Circuits Conference International Program Committee. He is currently an Associate Editor of the IEEE TRANSACTIONS ON BIOMEDICAL CIRCUITS AND SYSTEMS.